

Colon-Targeted Oral Delivery of Hydroxyethyl Starch-Curcumin Microcapsules Loaded with Multiple Drugs Alleviate DSS-Induced Ulcerative Colitis in Mice

Da Huang¹, Minglang Zou¹, Chenlan Xu¹, Yongming Wang, Zhenjin Xu, Wancong Zhang, Shijie Tang*, Zuquan Weng**

¹These authors contributed equally to this work.

D. Huang, M. Zou, C. Xu, Y. Wang, Z. Xu, Prof. Z. Weng

College of Biological Science and Engineering, Fuzhou University, Fuzhou, Fujian 350108, China.

Email: wengzq@fzu.edu.cn (Prof. Z. Weng)

W. Zhang, S. Tang

Department of Plastic Surgery and Burn Center, Second Affiliated Hospital, Shantou

University Medical College, Shantou, Guangdong 515051, China

Plastic Surgery Institute of Shantou University Medical College, Shantou, Guangdong 515051, China

Shantou Plastic surgery Clinical Research Center, Shantou, Guangdong 515051, China

E-mail: martine2007@sina.com (W.Z.); sjtang3@stu.edu.cn (S.T.)

Abstract

Combination therapy through colon-targeted oral delivery of multiple drugs presents a promising approach for effectively treating ulcerative colitis (UC). However, the co-delivery of drugs with diverse physicochemical properties in a single formulation remains a formidable challenge. In this study, we designed microcapsules based on hydroxyethyl starch-curcumin conjugates to enable the simultaneous delivery of hydrophobic dexamethasone acetate (DA) and hydrophilic cefazolin sodium (CS), yielding multiple drug-loaded microcapsules (CDHC-MCs) tailored for colon-targeted therapy of UC. Thorough characterization confirmed the successful synthesis and exceptional biocompatibility of CDHC-MCs. Biodistribution studies demonstrated that the microcapsules exhibited an impressive inflammatory targeting effect, accumulating preferentially in inflamed colons. *In vivo* experiments employing a dextran sulfate sodium (DSS)-induced UC mouse model revealed that CDHC-MCs not only arrested UC progression but also facilitated the restoration of colon length and alleviated inflammation-related splenomegaly. These findings highlight the potential of colon-targeted delivery of multiple drugs within a single formulation as a promising strategy to enhance UC treatment, and the CDHC-MCs developed in this study hold great potential in developing novel oral formulations for advanced UC therapy.

Keywords: microcapsules, hydroxyethyl starch-curcumin conjugates, ulcerative colitis, oral delivery, combination therapy

1. Introduction

Inflammatory bowel disease is a complex and chronic ailment characterized by multifaceted gastrointestinal inflammation ^[1]. Within the spectrum of inflammatory bowel disease, two predominant manifestations exist: Crohn's disease (CD) and ulcerative colitis (UC). UC, in particular, embodies a recurring inflammatory state predominantly affecting the distal segments of the intestinal tract ^[2,3]. This condition is typified by the persistence of intestinal inflammation and consequential destruction of the colonic epithelium ^[4]. UC is a widespread affliction, affecting millions of individuals worldwide, with an escalating global prevalence, notably in regions of historically lower incidence ^[5]. Contemporary pharmacotherapy for UC primarily relies on a repertoire of medications, including amino salicylates, corticosteroids, and immunosuppressants ^[6-8]. However, these drugs are limited by their unsatisfactory therapeutic effects owing to low bioavailability and unfavorable pharmacokinetic properties, often accompanied by a range of adverse side effects ^[9]. Therefore, the development of alternative drug formulations with improved therapeutic efficacy and minimal side effects is of critical importance.

While the exact pathogenesis of UC remains unclear, accumulating evidence indicates that the etiology of UC is intricately linked to multiple mechanisms, including dysregulated inflammatory responses ^[10], oxidative stress ^[11, 12], and intestinal dysbiosis ^[13], caused by genetic and/or environmental factors. Given the multifactorial nature of UC, monotherapy often proves inadequate in achieving optimal outcomes ^[14]. In recent years, there has been a growing exploration of combination therapies that combine traditional pharmaceuticals with innovative approaches targeting various aspects of UC pathophysiology ^[15, 16]. For example, research has shown that the combination of dexamethasone acetate (DA), a commonly prescribed anti-inflammatory corticosteroid for UC, with natural polyphenols such as curcumin (CUR) and tannic acid can achieve a synergistic effect in UC therapy ^[17, 18]. CUR, a hydrophobic polyphenol derived from turmeric, is particularly promising for its potential to regulate inflammation and alleviate oxidative stress ^[19]. Additionally, CUR has been found to modulate the intestinal microbiota, inhibit the inflammatory transcription factor NF-kappa B, and positively influence intestinal health and permeability ^[20]. Moreover, the administration of

antibiotics or probiotics, such as cefazolin sodium (CS)^[21], with proven antibacterial efficacy against Gram-positive bacteria, has been shown to be beneficial in UC treatment, as UC patients often face complications related to intestinal bacterial infections due to chronic diarrhea, mucosal ulceration, and compromised mucosal resistance^[22]. However, the systemic administration of these drugs, due to their nonspecific delivery mechanisms, is fraught with issues of low bioavailability and potential side effects, thus limiting the exploration of combination therapy efficacy^[23, 24]. Consequently, the development of novel drug delivery systems capable of concurrently delivering multiple therapeutic agents while targeting the colon represents a critical clinical imperative in enhancing UC treatment.

Remarkably, advancements in micro/nanotechnology have ushered in a paradigm shift in UC treatment. These innovations leverage the epithelial enhanced permeability and retention (eEPR) effect to precisely target inflammatory tissues^[25, 26]. Micro/nanoparticles can passively accumulate within inflamed colonic tissues, exploiting increased vascular network permeability, disruptions in intercellular connections, and mucous layer damage^[27]. Furthermore, the UC microenvironment, characterized by reduced pH levels, heightened levels of reactive oxygen species, and overexpressed enzymes (α -amylase, neutrophil elastase, myeloperoxidase, etc.)^[28-30], renders micro/nano carriers responsive to these stimuli, promising highly specific drug delivery in UC therapy. Previously, we reported the development of α -amylase-responsive micelles based on hydroxyethyl starch-curcumin (HES-CUR) conjugates for colon-targeted co-delivery of DA and CUR^[18]. This nanoparticle-based formulation demonstrated enhanced therapeutic efficacy in mitigating UC-induced lesions through colon-targeted combination therapy. Nevertheless, micelles can only encapsulate hydrophobic drugs such as DA. The incorporation of multiple drugs, including hydrophobic DA and hydrophilic CS, within one drug delivery system remains challenging.

In contrast to micelles, microcapsules fabricated from hydrophobic polymers represent a class of micro/nano carriers with the capacity to encapsulate both hydrophobic and hydrophilic drugs simultaneously^[31]. This is achieved by encapsulating hydrophobic drugs in the hydrophobic wall and hydrophilic drugs in the inner cavity of the microcapsules. Moreover, microcapsules offer the advantages of facile preparation and scalability^[32]. In this study, we prepared

hydrophobic HES-CUR conjugates by conjugating numerous CUR molecules onto HES. Subsequently, HES-CUR microcapsules were fabricated using a water-in-oil-in-water (W/O/W) double emulsion method, and both DA and CS were simultaneously loaded into the microspheres to obtain CD/DA-loaded HES-CUR microcapsules (CDHC-MCs). CDHC-MCs are specifically tailored for colon-targeted delivery of DA and CS, offering a comprehensive therapeutic approach to UC. As delineated in **Figure 1**, orally administered CDHC-MCs can accumulate in inflamed colonic tissues via the eEPR effect. Subsequently, the α -amylase-mediated degradation of the microspheres results in the release of multiple drugs in the inflamed colon, leading to a synergistic therapeutic effect mediated by CUR, DA, and CS. The morphology, zeta potential, and drug-loading capacity of the CDHC-MCs were characterized, and their biocompatibility was evaluated by measuring their cytotoxicity against 3T3-L1 cells. Animal experiments conducted in mice with dextran sulfate sodium (DSS)-induced UC were performed to evaluate the colon-targeting effect and therapeutic effect of the CDHC-MCs.

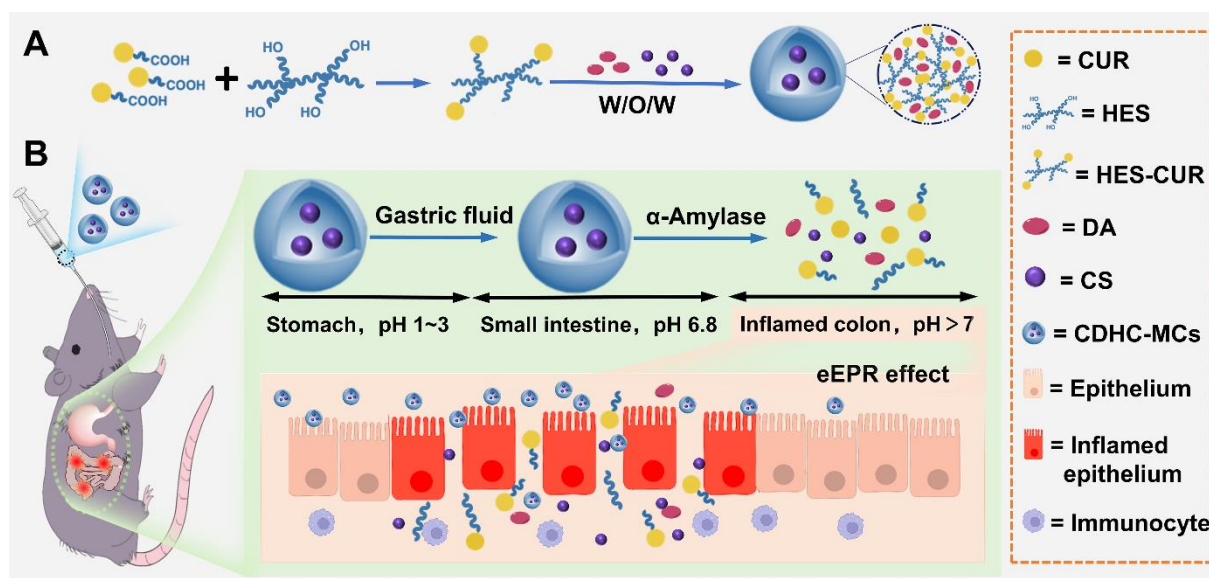


Figure 1. Schematic illustration of fabrication and oral drug delivery process of DCHC-MCs.

2. Results and Discussion

2.1. Synthesis of HES-CUR Conjugates

The synthesis of HES-CUR conjugates was achieved following the synthetic route presented in **Figure 2A**. To facilitate the esterification of CUR with HES, CUR-COOH was initially synthesized to reduce steric hindrance. Then the esterification of the carboxyl group of CUR-

COOH with the hydroxyl group of HES produced HES-CUR conjugates. The successful synthesis of HES-CUR conjugates was confirmed by ^1H NMR spectrum. As shown in **Figure 2B**, the peaks associated with carboxyl groups of CUR-COOH vanished in the ^1H NMR spectrum of HES-CUR. In contrast, the peaks corresponding to CUR (9.67 ppm, 6.15-7.58 ppm) and HES (3.54 ppm, 3.66 ppm, 4.57-5.22 ppm) were clearly detected. These findings confirmed the successful synthesis of HES-CUR conjugates.

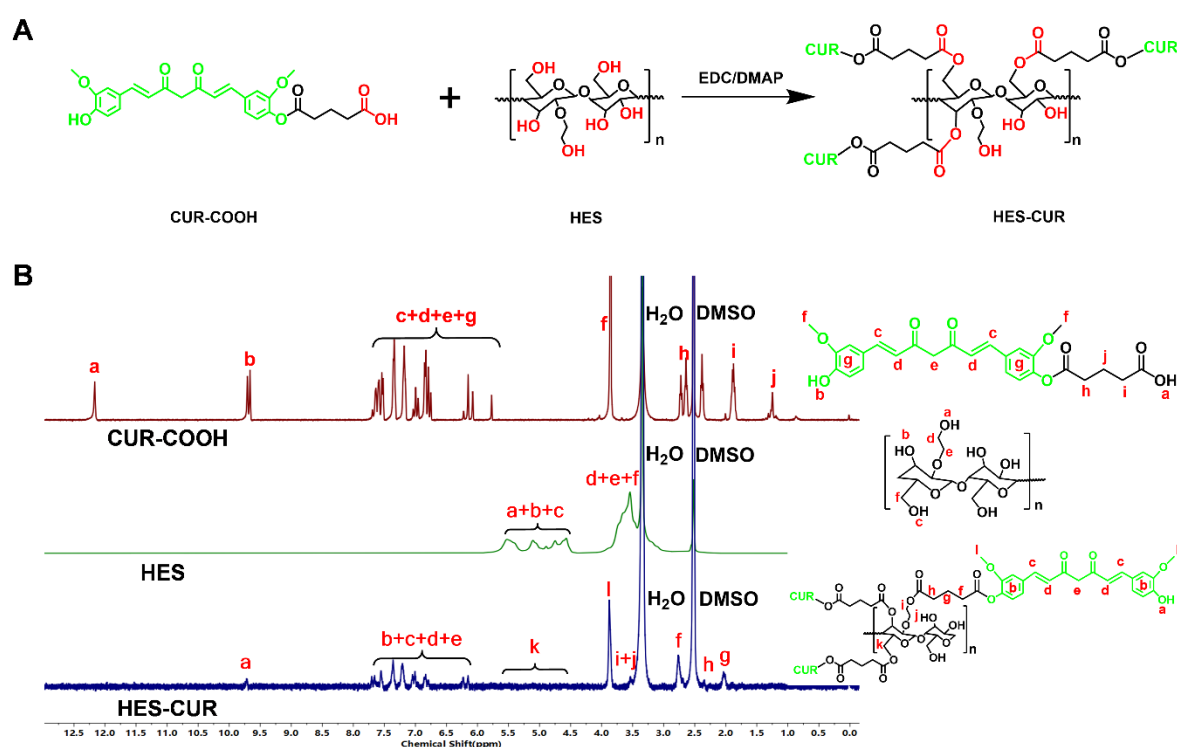


Figure 2. Synthesis of HES-CUR conjugates. (A) Synthetic route of HES-CUR conjugate. (B) ^1H NMR spectra of CUR-COOH, HES and HES-CUR conjugate.

2.2. Preparation and Characterization of CDHC-MCs

CDHC-MCs were prepared via a W/O/W double emulsion method, resulting in microcapsules with spherical shapes, continuous surfaces, and no noticeable cracks or fractures, as revealed in the SEM image (**Figure 3A**). After ultrasonic fragmentation, the broken CDHC-MCs exhibited a concave shape inside, confirming that the particles were hollow (inset in **Figure 3A**). The average hydrodynamic size of the CDHC-MCs determined by DLS was $3.96 \pm 2.26 \mu\text{m}$ (**Figure 3B**), in accordance with the size observed in the SEM image. Zeta potential analysis indicated

that the surface charge of CDHC-MCs was -26.59 ± 0.73 mV (**Figure 3C**). This negative surface charge conferred favorable colloid stability by preventing aggregation through electrostatic repulsion^[33]. Importantly, it was reported that the inflamed colon mucosa typically exhibits positive charge due to the presence of positively charged proteins such as transferrin and antimicrobial peptides^[34], hence the negatively charged nature of the CDHC-MCs may facilitate their accumulation in the inflamed colon.

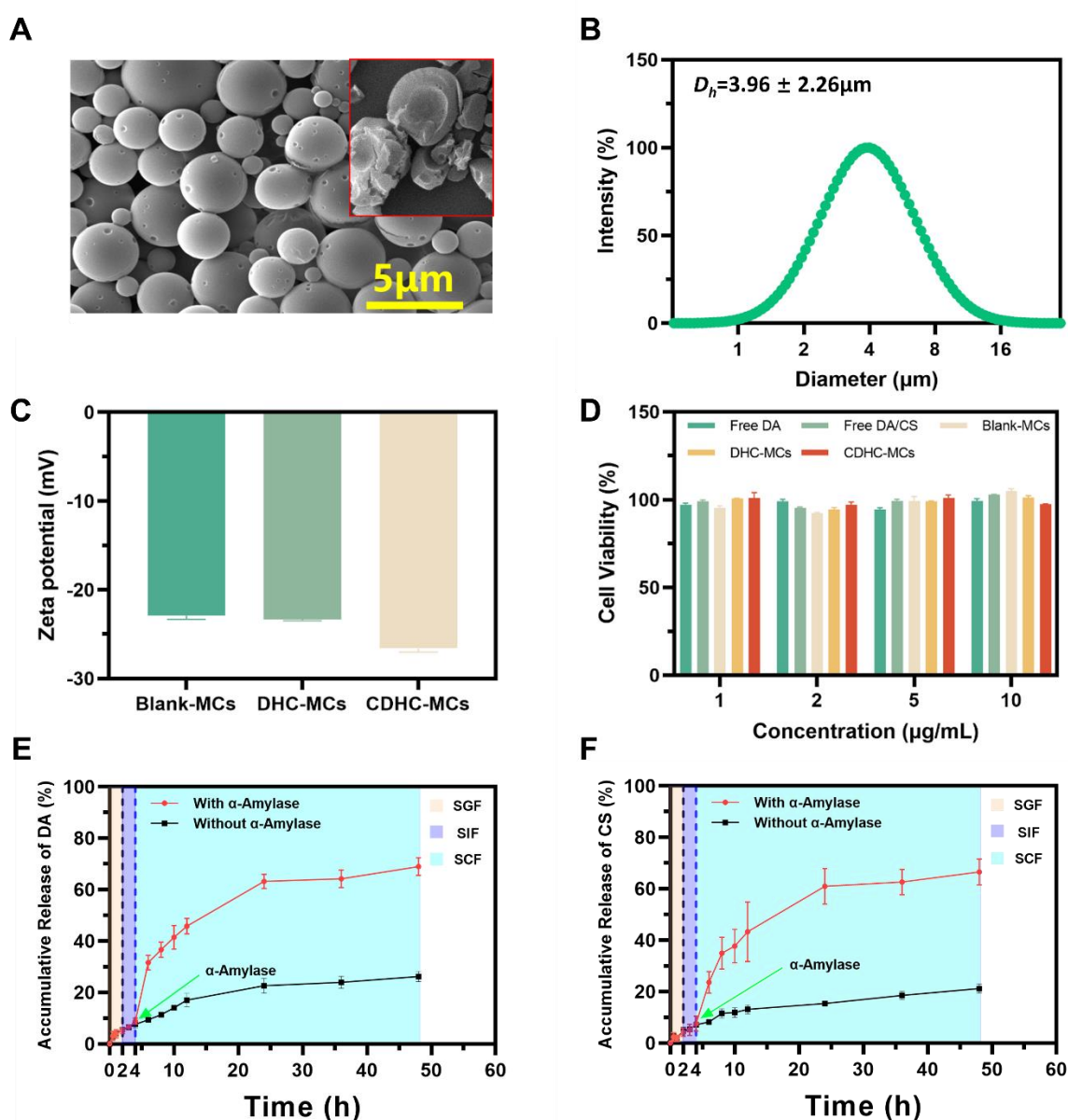


Figure 3. Characterization of CDHC-MCs. (A) SEM images of CDHC-MCs (Inset: Broken microcapsules after ultrasonic fragmentation). (B) Size distributions and (C) Zeta potential of CDHC-MCs. (D) Cell viabilities of 3T3-L1 cells after incubation with free DA, free DA/CS,

Blank-MCs, DHC-MCs and CDHC-MCs for 24 h. Accumulative release profiles of (E) DA and (F) CS from CDHC-MCs in oral administration microenvironment.

The loading efficiencies for CUR, DA, and CS were determined to be 39.16%, 10.95%, and 0.77%, respectively, with encapsulation efficiencies for DA and CS amounting to 11.45% and 35.38%, respectively. This represents a significant enhancement in the loading efficiencies of CUR and DA compared to DA-loaded HES-CUR micelles reported previously^[18], where the loading efficiency for CUR increased from 13.3% to 39.16% and for DA from 2.7% to 10.95%. This improvement can be attributed to the relatively hydrophobic nature of the HES-CUR conjugates used in this study. The preparation of micelles involves self-assembly of amphiphilic polymers, which limits CUR loading efficiency due to the necessity for a delicate hydrophilic/hydrophobic balance. Furthermore, the low hydrophobic area within the micelles restricted loading of hydrophobic DA. In contrast, microcapsules, which can be prepared using highly hydrophobic polymers, allow for increased conjugation degree of CUR onto HES in this study. Benefitting from the relatively high hydrophobicity, the DA can be encapsulated in the hydrophobic wall of the microcapsules with high loading efficiency via hydrophobic interaction.

2.3. *In vitro* release of DA and CS from CDHC-MCs

In vitro release studies were conducted sequentially in simulated gastric fluid (SGF, pH = 1.2), simulated small intestinal fluid (SIF, pH = 6.8), and simulated colon fluid (SCF, pH = 7.4) to mimic the drug release profile of CDHC-MCs in the oral administration microenvironment. To investigate the responsiveness of CDHC-MCs to α -amylase, we also monitored their release behavior in SCF with and without α -amylase. Given that orally administered formulations typically spend approximately 2-4 h in the human stomach and small intestine, and 12-48 h in the colon^[24], we tracked the release of DA and CS from CDHC-MCs for 2 h in SGF and SIF, respectively, followed by 44 h in SCF. As shown in **Figure 3E** and **Figure 3F**, CDHC-MCs released less than 10% of DA and CS during the initial 4 h, suggesting that the microcapsules can protect the encapsulated drugs from release before reaching the colon. Over the subsequent 44 h, the release of DA and CS gradually reached approximately 26% and 20%, respectively, in the α -amylase-free SCF. In contrast, the presence of α -amylase in SCF significantly accelerated the release of both drugs, resulting in over 65% cumulative release. This disparity

can be attributed to the hydrolysis of HES in CDHC-MCs by α -amylase, leading to the structural disintegration of the microcapsules and subsequent release of encapsulated drugs. Considering the elevated α -amylase levels in the colon of UC patients ^[18], CDHC-MCs offer a promising approach for achieving colon-specific drug delivery.

2.4. Cytotoxicity of CDHC-MCs

Given that CDHC-MCs are orally administered and interact directly with the internal environment of the human body, assessing their biocompatibility is crucial. In this study, the cytocompatibility of free DA, free DA/CS, Blank-MCs, DHC-MCs, and CDHC-MCs was assessed by CCK-8 assay using 3T3-L1 cells as a normal cell model. As illustrated in **Figure 3D**, within the concentration range of 1-10 $\mu\text{g/mL}$ and after 24 h of treatment, cell viability exceeded 80% in all groups. This finding suggested that the microcapsule formulations prepared in this study exhibited excellent biocompatibility. This outcome aligned with expectations, given that the raw materials used in the synthesis of CDHC-MCs primarily derive from natural sources, such as CUR and HES, both of which have demonstrated exceptional biocompatibility in prior studies, as well as in the present study ^[18, 35].

2.5. Inflammatory Targeting Effect of CDHC-MCs

As previously mentioned, microcapsules exhibit a significant inflammation-targeting effect, allowing them to accumulate in the inflamed colon through the eEPR effect and improved mucosal penetration (**Figure 1B**) ^[25, 36]. Moreover, microcapsules possessing a negative charge are predisposed to preferentially target UC. This preference stems from the positively charged nature of the inflamed colonic epithelium, attributed to the accumulation of positively charged proteins, including eosinophil cationic protein, transferrin, and antimicrobial peptides ^[34, 37]. Consequently, we hypothesized that CDHC-MCs with their negative charge could effectively target colitis.

To validate this hypothesis, IHC-MCs labeled with near-infrared dye IR-780 were orally administered to mice with or without DSS-induced UC, and subsequently the biodistribution of IHC-MCs was monitored. As shown in **Figure 4A**, fluorescence of IHC-MCs was observed in the abdominal area of mice at 3 h, 10 h, and 24 h post-administration. Notably, the fluorescence

intensity in the Healthy group was much weaker than that in the DSS group after 24 h. The quantitative analysis of fluorescence intensity (**Figure 4B**) further confirmed that the average fluorescence intensity in the DSS group was significantly higher than that in the Healthy group at the 24 h mark, aligning with our visual observations.

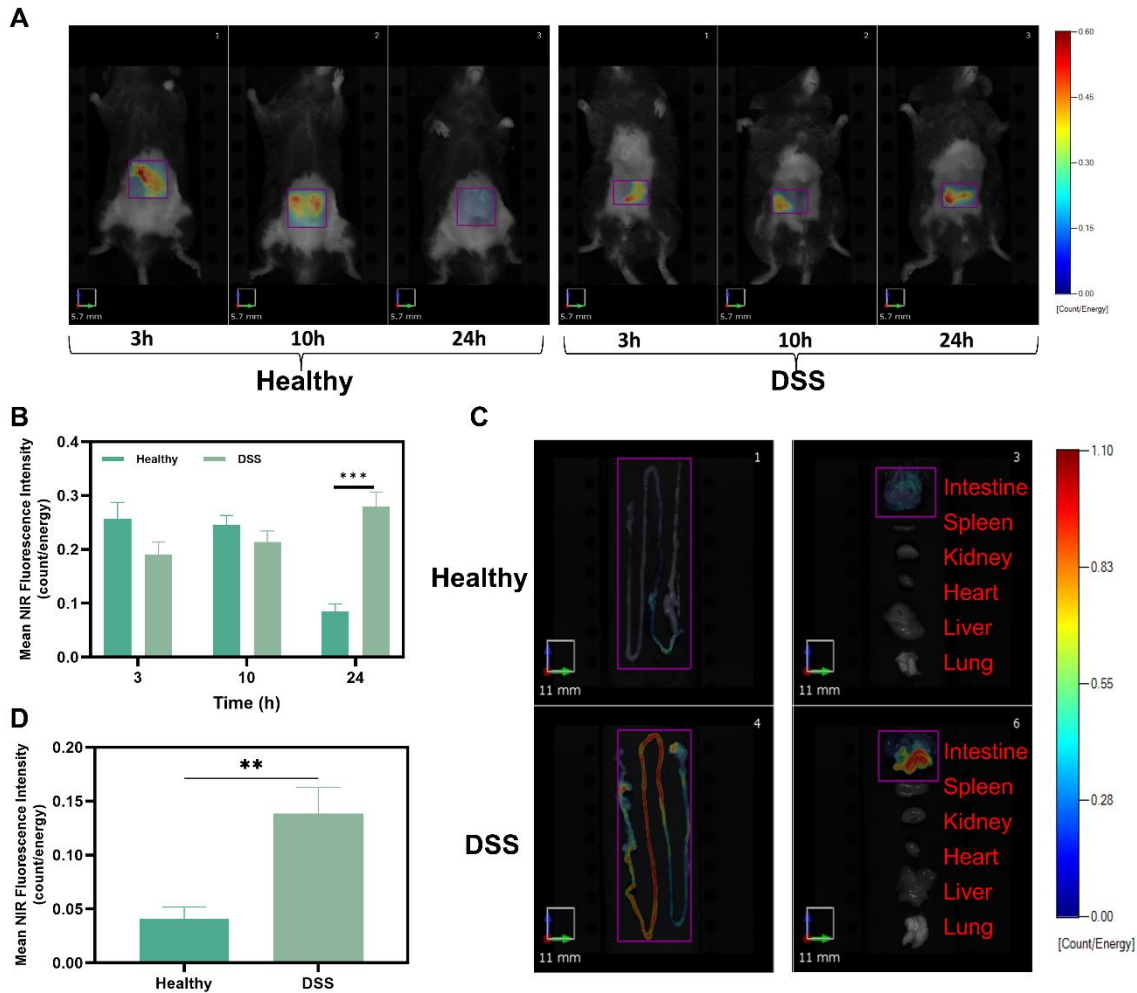


Figure 4. Biodistribution of IHC-MCs in mice with or without DSS-induced UC. (A) Fluorescence images of mice after orally administered IHC-MCs for different hours. (B) Quantitative analysis of fluorescence intensities at the regions of interest. Statistical analysis was performed by unpaired Student's t-test (two-tailed), and data were expressed as the mean \pm SD ($n = 6$), *** $P < 0.001$. (C) Fluorescence images of colons and major organs extracted from mice after orally administered IHC-MCs for 24 h. (D) Quantitative analysis of fluorescence intensities at the colons. Statistical analysis was performed by unpaired Student's t-test (two-tailed), and data were expressed as mean \pm SD ($n = 6$), ** $P < 0.01$.

After 24 h of intragastric administration, the mice were euthanized, and various organs including the colons, spleens, kidneys, hearts, livers, and lungs were collected and imaged. As demonstrated in **Figure 4C**, strong fluorescence was observed in the colons of the DSS group in comparison to the Healthy group, with no detectable fluorescence in the spleens, kidneys, hearts, livers, and lungs in either group. Quantitative analysis further confirmed that the average fluorescence intensity in the colon of the DSS group was significantly higher than that in the Healthy group (**Figure 4D**). Collectively, these results provide compelling evidence that formulations based on CDHC-MCs possess the capability to accumulate in inflamed colon tissue and hold promise for targeted drug delivery in UC therapy.

2.6. *In vivo* Therapeutic Effect of CDHC-MCs Against DSS-Induced UC

Encouraged by the results from the biodistribution study, we further investigated the therapeutic effect of CDHC-MCs using mice with DSS-induced UC. As outlined in **Figure 5A**, the UC model was created by administration of 3% DSS solution for 7 days, then on the 8th day, the mice with UC were divided into 5 groups and treated with distilled water, free DA/CS, Blank-MCs, DHC-MCs, and CDHC-MCs, respectively. One group of mice without any treatment throughout the experiment was set as Healthy control.

Clinical characteristics of UC included weight loss, diarrhea, and hematochezia. To gauge the severity of UC, daily monitoring of body weight and the calculation of the DAI score based on alterations in weight, fecal consistency, and hematochezia were conducted. Higher weight loss and DAI scores indicated more severe UC ^[38]. As demonstrated in **Figure 5B**, during the establishment of UC over the initial 7 days, the body weight of all DSS groups exhibited a rapid decline, confirming the successful induction of UC. Subsequently, during the following 7 days, alterations in body weight in various treatment groups reflected the efficacy of different formulations. The rate of weight loss decelerated in all treatment groups, with CDHC-MCs halting weight loss or even restoring it to near the initial body weight after 3 days of treatment, while the DSS group continued to experience declining body weight. Furthermore, all microcapsule-based formulations exhibited superior effectiveness in reducing weight loss compared to free DA/CS. Statistical analysis revealed that the therapeutic effect of the CDHC-

MCs group was significantly enhanced in comparison to the DSS group and the free DA/CS group at the end of treatment. Similar results were observed in the DAI scores (Figure 5C). The DAI score of the DSS group exhibited a significant increase and subsequently decreased to varying degrees after the administration of different formulations. Notably, the DAI score of the CDHC-MCs group was significantly lower than that of the DSS group and the free DA/CS group, further substantiating the superiority of CDHC-MCs in the treatment of UC. The improved therapeutic effect may be attributed to the increased accumulation of the microcapsules in the inflamed colon.

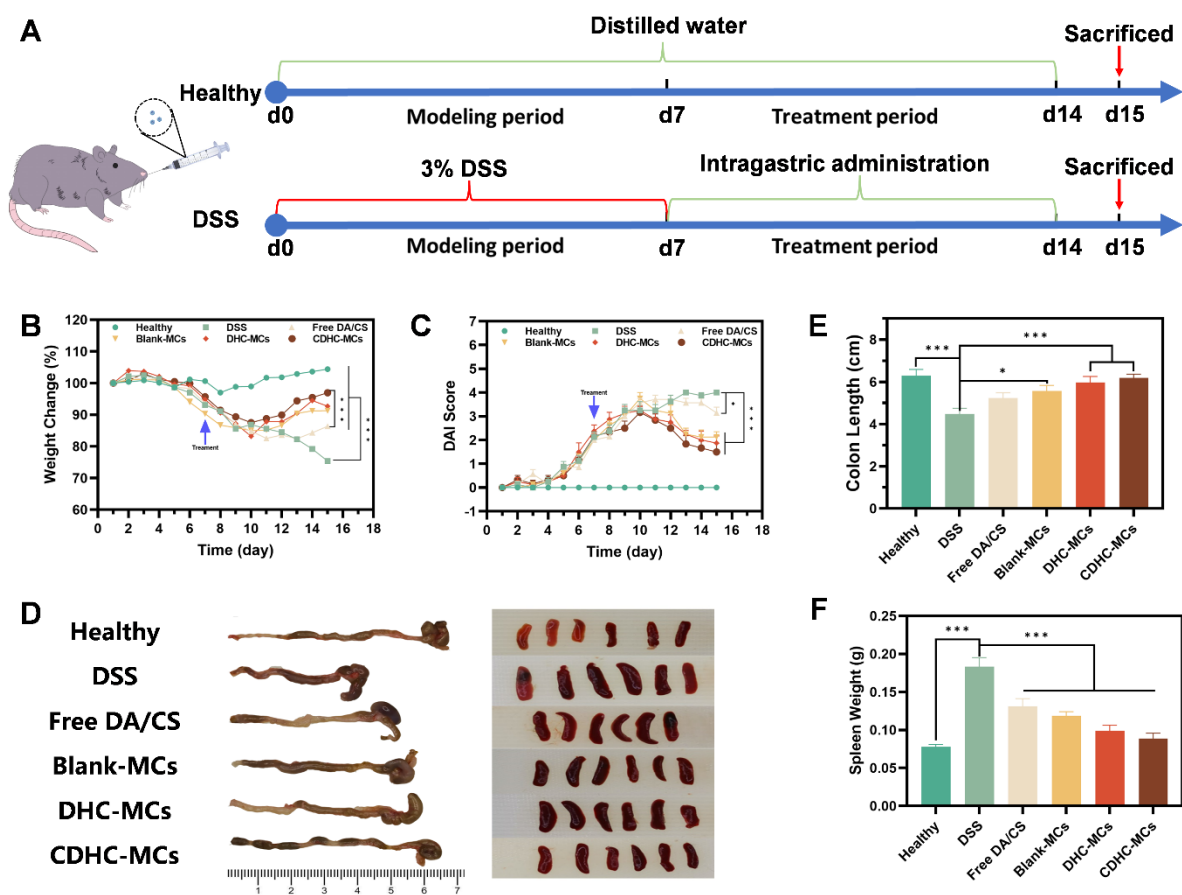


Figure 5. *In vivo* evaluation of the therapeutic effect of CDHC-MCs against DSS-induced UC. (A) Schematic representation of animal experimentation protocol. (B) Weight loss and (C) DAI scores of mice with different treatments. Statistical analysis was performed by one-way ANOVA followed by Tukey’s post hoc test, and data were expressed as the mean \pm SD (n = 6), *P < 0.05, ***P < 0.001. (D) Colons and spleens extracted from mice with different treatments. Quantitative analysis of (E) colon length and (F) spleen weight of mice with different

treatments. Statistical analysis was performed by one-way ANOVA followed by Tukey's post hoc test, and data were expressed as mean \pm SD ($n = 6$), * $P < 0.05$, *** $P < 0.001$.

Colon length serves as a reflection of the pathological severity of colitis, because scar tissue at inflammatory sites leads to shortening of the colon^[39]. As shown in **Figure 5D**, compared to the treatment groups, the colons of the DSS group exhibited the shortest length. However, the treatment with different formulations preserved colon length in different degrees, and the UC mice treated with CDHC-MCs exhibited the best recovery in colon length, approaching that of healthy mice. Further quantitative analysis revealed a significant difference in colon length between the groups treated with microcapsule formulations and the DSS group, while no significant difference was observed between the free DA/CS group and the DSS group (**Figure 5E**). This indicates that oral administration of CDHC-MCs can ameliorate colon shortening attributed to scar formation and the microcapsules enhanced the therapeutic effect of free drugs.

The spleen, being the largest immune and lymphoid organ in mice, plays a pivotal role in the immune response involving lymphocytes and macrophages and is known to enlarge in response to inflammation^[40]. To evaluate the severity of inflammation, spleen weights were measured at the end of treatment. As shown in **Figure 5D**, the spleens of the DSS group were significantly larger than those in the treatment groups, while the size of the spleen in the CDHC-MCs group closely resembled that of the Healthy group. Subsequent statistical analysis revealed a decrease in spleen weight in the following order: Free DA/CS, Blank-MCs, DHC-MCs, and CDHC-MCs (**Figure 5F**), indicating the formulations relieved inflammation and the CDHC-MCs exhibited the best anti-inflammatory effect.

Subsequently, colon sections from each group were subjected to pathological analysis. The H&E-stained colon sections presented in **Figure 6**, provide a direct representation of the extent of colonic lesions. The colon section from healthy mice demonstrated the normal structure of colon tissue, with neatly arranged goblet cells and intact, well-defined colonic mucosa (**Figure 6A**). In contrast, the colon section from mice with UC exhibited extensive epithelial destruction, characterized by significant interstitial edema and a significant loss of goblet cells (**Figure 6B**). Treatment with different formulations helped restore intestinal mucosa structure to varying

degrees (**Figure 6C-F**). Importantly, colon sections from CDHC-MCs treated mice exhibited intact and continuous mucosal epithelium, well-organized goblet cells, and an absence of inflammatory cell infiltration, hyperemia, or edema (**Figure 6F**). These histological results affirm that CDHC-MCs treatment effectively mitigated the inflammatory damage caused by DSS-induced UC.

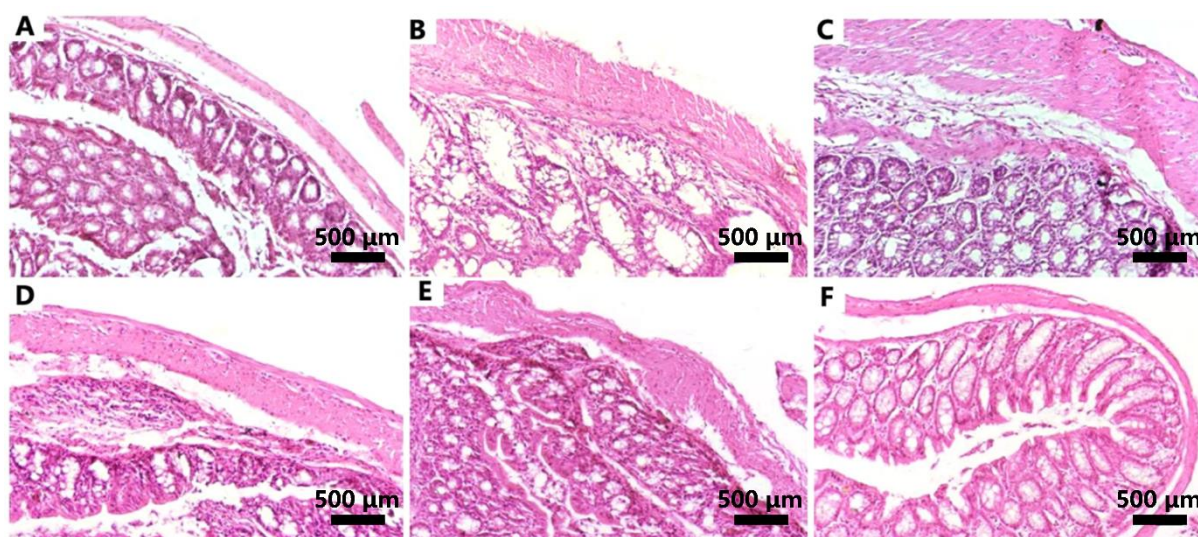


Figure 6. Representative images of H&E-stained colon sections from various groups. (A) Healthy control group, (B) DSS control group, (C) Free DA/CS-treated DSS group, (D) Blank-MCs-treated DSS group, (E) DHC-MCs-treated DSS group and (F) CDHC-MCs-treated DSS group (E). Images of tissues are shown at 200×magnification.

3. Conclusion

In summary, this study presents the development of a multiple-drug loaded microcapsule formulation for treatment of UC. Through the use of micro/nanotechnology, we have successfully developed CDHC-MCs capable of loading various drugs with different physicochemical property for colon-targeted oral delivery in UC therapy. Through extensive characterization, we demonstrated the successful fabrication and excellent biocompatibility of CDHC-MCs, in addition to their remarkable inflammatory targeting effect, as evidenced by their preferential accumulation in inflamed colons. Moreover, *in vivo* experiments in a DSS-induced UC mouse model showcased the substantial therapeutic potential of CDHC-MCs, which not only effectively halted the progression of UC but also facilitated the restoration of colon length and minimized inflammation-associated splenomegaly. The enhancement in drug

loading efficiency further underscores the potential of CDHC-MCs as a transformative platform to address the multifaceted challenges associated with UC. The CDHC-MCs presented in this study hold promise in developing novel oral formulations for advanced UC therapy.

4. Experimental Section

Materials: CUR (95%), glutaric anhydride (GA, 99%), 4-dimethylaminopyridine (DMAP, 98%), N-ethyl-N'-[3-(dimethyl amino) propyl] carbodiimide hydrochloride (EDC, 98%), and near-infrared dye IR780 (99%) was sourced from Energy Chemical (Shanghai, China). HES with a molar substitution of hydroxyethyl of 0.5 and an average molecular weight of 200 kDa was obtained from Wuhan HUST Life Science & Technology Co, Ltd. (Wuhan, China) and dried at 60 °C for 12 h prior to use. DA (98%) and CS (98%) were procured from Aladdin Industrial Corporation (Shanghai, China) and used without further purification. DSS (colitis grade, molecular weight 360 ~ 500 kDa) was acquired from MP Biomedicals (Santa Ana, California, USA). Dulbecco's modified Eagle medium (DMEM) and fetal bovine serum (FBS) were obtained from Gibco. CCK-8 solution was purchased from Meilunbio (Da Lian, China). All other reagents used in this study were of analytical grade and used as received.

Synthesis of HES-CUR Conjugates: HES-COOH was firstly synthesized following our previously report^[18]. CUR (17.68 g) was dissolved in anhydrous pyridine and stirred at room temperature for 15 minutes. Subsequently, a solution of glutaric anhydride (5.48 g) in anhydrous pyridine was slowly added to the reaction vessel, and the mixture was stirred in the dark at room temperature for 7 h. The organic layer was extracted with ethyl acetate and HCl. The crude CUR-containing product was obtained through drying and rotary evaporation under reduced pressure. Finally, CUR-COOH was purified using silica gel column chromatography with dichloromethane/methanol (100:1, v/v) as eluent and dried overnight under vacuum at 30 °C.

The aforementioned CUR-COOH (2.61 g) was dissolved in anhydrous dimethyl sulfoxide. Then, EDC (207 mg) and DMAP (66 mg) were added and stirred at room temperature for 30 minutes. HES (160 mg), dissolved in anhydrous dimethyl alum, was slowly added to the reaction solution, and the mixture was stirred in the dark for 48 h at room temperature. The reaction mixture was slowly added to an ethanol/ether mixture, and the precipitate was collected

by centrifugation at 10,000 rpm for 10 minutes. The resulting precipitate was re-dissolved in dimethyl sulfoxide, dialyzed against water for 72 h (MWCO: 3500 Da), and freeze-dried to obtain HES-CUR.

Preparation and Characterizations of CDHC-MCs: CDHC-MCs were prepared via a water-in-oil-in-water (W/O/W) double emulsion method. Briefly, HES-CUR (50 mg) and DA (2 mg) were dissolved in a mixture of dichloromethane (4.5 mL) and dimethyl sulfoxide (0.5 mL) with the assistance of ultrasound, serving as the oil phase (O). Then 1 mL solution of CS at a concentration of 50 $\mu\text{g mL}^{-1}$ was slowly added to the oil phase, and ultrasonication for 1 minute generated the initial water-in-oil (W/O) emulsion. This primary emulsion was introduced into a 40 mL 2% PVA solution as the external water phase, creating the water-in-oil-in-water emulsion (W/O/W) through overnight stirring at room temperature. Lastly, CDHC-MCs were obtained by centrifugation, washing, and freeze drying.

Furthermore, Blank-MCs were prepared without DA and CS, while DA-loaded HES-CUR microcapsules (DHC-MCs) were produced by replacing the inner aqueous phase CS solution with an equivalent volume of ultra-pure water, with all other steps identical to those mentioned above. Similarly, IR780-loaded HES-CUR microcapsules (IHC-MCs) were prepared for the biodistribution study.

The morphology of CDHC-MCs was observed using scanning electron microscopy (SEM, Quanta 250, FEI, USA) after coating with platinum. The hydrodynamic diameter and size distribution of the CDHC-MCs were measured by dynamic light scattering (DLS) using a zeta potential and granularity analyzer (Omni, Brookhaven, USA) after the freeze-dried microcapsules were dispersed in ultra-pure water with a concentration of 1 mg mL^{-1} .

To validate the hollow structure of the CDHC-MCs, a suspension of CDHC-MCs (1 mg mL^{-1}) was treated with ultrasound (Power: 100 W) for 10 minutes to induce their rupture. The resulting suspension was subsequently freeze-dried and examined using SEM.

Determination of Loading and Encapsulation Efficiency of Drugs in CDHC-MCs: To measure the loading efficiency of CUR, HES-CUR conjugates were weighed and dissolved in a HCl/DMSO (1:4, v/w) mixed solution with ultrasonication for 4 h at room temperature to ensure

completely detachment of CUR. The absorbance of the solution was measured at 425 nm using a microplate reader (Synergy H1, USA) and CUR's quantity was determined based on a standard curve.

To measure the loading and encapsulation efficiency of DA and CS, freeze-dried CDHC-MCs were dissolved in methanol, followed by filtration through a 0.22 mm membrane after 1 h of sonication. High-performance liquid chromatography (HPLC, Thermo Ultimate 3000, USA) was employed to assess the drug concentration (CS and DA) in the solution at a detection wavelength of 273 nm for CS and 240 nm for DA. The mobile phase consisted of a mixture of methanol and ultra-pure water (7:3, v/v) at a flow rate of 1.00 mL min⁻¹. Then the loading and encapsulation efficiencies were calculated based on the obtained drug concentrations.

In vitro release of DA and CS from CDHC-MCs: The *in vitro* release profiles of DA and CS from CDHC-MCs were evaluated in sequential stages using SGF, SIF and SCF. Initially, CDHC-MCs were dispersed in PBS with a concentration of 1 mg mL⁻¹. Subsequently, 1 mL of the suspension was transferred to a dialysis tube with a molecular weight cut-off of 3500 Da. The dialysis tube was immersed in SGF for the initial 2 h, followed by SIF for the subsequent 2 h. The release medium was then replaced with SCF, both with and without α -amylase (0.064 KNU/mL), for the following 44 h. The release medium was incubated at 37°C with shaking (100 rpm). At pre-determined intervals, 1 mL of release medium was sampled, and an equivalent volume of fresh medium was replenished. The concentration of DA and CS in the samples was determined by HPLC, and the cumulative release was subsequently calculated. The experiments were conducted in triplicate.

Cytotoxicity Assay: Mouse embryonic fibroblasts 3T3-L1 cells were cultured in a medium containing DMEM, 10% FBS, and 1% penicillin/streptomycin at 37 °C in 5% CO₂. The cells were seeded into 96-well plates at a density of 5000 cells per well and incubated in a cell incubator for 24 h. Subsequently, the cells were exposed to various treatments, including DA, DA/CS, Blank-MCs, DHC-MCs, and CDHC-MCs, for 24 h, with final DA concentrations ranging from 0.5 to 10 $\mu\text{g mL}^{-1}$ and CS concentrations from 0.007 to 0.7 $\mu\text{g mL}^{-1}$. The control group received culture medium alone. After 24 h of exposure, the culture medium was removed,

and the wells were washed twice with phosphate-buffered saline (PBS). Next, 100 μL of complete medium containing 10% CCK-8 was added to each well and incubated for 2 h. The absorbance at 450 nm was measured for each well. Cell viability was calculated by comparing the absorbance of treated wells to that of control wells without treatment.

Animals: Male C57BL/6 mice weighing between 22-24g were used for *in vivo* studies. These mice were maintained under specific pathogen-free (SPF) conditions with a room temperature of 20-25°C, relative humidity of 40%-60% and a 12 h light/dark cycle, provided with distilled water and food. All experiments performed on the mice comply with the protocol ((NO. 2023-SG-006) which was approved by the Institutional Animal Care and Use Committee of Fuzhou University. To induce the UC model, the mice's drinking water was replaced with a 3% (w/v) DSS solution for seven consecutive days.

Biodistribution: On the 7th day of the experiment, both groups of mice (6 mice in each group) underwent abdominal depilation and were fasted without access to water. On the following day, they were orally administered 400 μL of IHC-MCs suspension. After 3, 10, and 24 h, the mice were anesthetized with isoflurane for *in vivo* imaging. Following 24 h of *in vivo* imaging, the mice were euthanized by CO_2 , and their hearts, livers, spleens, lungs, kidneys, and intestines were collected for organ imaging using an *in vivo* near-infrared imaging system (In-Vivo Master, Grand-imaging Technology Co., Ltd, Wuhan, China).

In vivo Therapeutic Effect Against DSS-Induced UC: On the 8th day of the experiment, groups of mice with induced UC (6 mice in each group) received daily oral gavage of the following treatments for 7 days: free DA/CS solution (2/0.14 mg kg^{-1}), Blank-MCs (13.3 mg kg^{-1}), DHC-MCs (17.5 mg kg^{-1}), and CDHC-MCs (18.3 mg kg^{-1}). Healthy mice and those receiving only DSS were given water. Daily assessments included monitoring body weights and disease activity index (DAI) scores, which were calculated based on weight loss, stool consistency, and stool bleeding, as described in a prior report.

Upon completing the treatment period, the mice were euthanized using CO_2 , and their spleen weights and colon lengths were measured. Subsequently, colon segments were fixed in formalin

and embedded in paraffin. The colon samples were then sectioned at a thickness of 5 μm and stained with hematoxylin and eosin (H&E) for histological analysis.

Statistical analysis: Data were presented as mean \pm SD. Unpaired Student's t-test (two-tailed) was used to compare mean values of two groups. One-way analysis of variance (ANOVA) followed by Tukey's post hoc analysis was used for the comparison of means of three or more groups. * $P < 0.05$ was considered to have a significant difference. The plotting and statistical analysis were performed using GraphPad Prism 9.5.0 software.

Acknowledgements

D. Huang, M. Zou and C. Xu contributed equally to this work. The authors acknowledgment the financial support from the National Natural Science Foundation of China (81971837), and the Natural Science Foundation of Fujian Province (2023J01410).

Conflict of Interest

The authors declare no conflict of interest.

Received: ((will be filled in by the editorial staff))

Revised: ((will be filled in by the editorial staff))

Published online: ((will be filled in by the editorial staff))

References

- [1] M. A. Engel, M. F. Neurath, *J. Gastroenterol.* **2010**, *45*, 571.
- [2] Y. R. Yu, J. R. Rodriguez, *Semin. Pediatr. Surg.* **2017**, *26*, 349.
- [3] C. Liu, Q. Wang, Y.-L. Wu, *Macromol. Biosci.* **2023**, 2300157.
- [4] T. Ahmad, C. Pesi Tamboli, D. Jewell, J.-F. Colombel, *Gastroenterology* **2004**, *126*, 1533.
- [5] I. Ordas, L. Eckmann, M. Talamini, D. C. Baumgart, W. J. Sandborn, *Lancet* **2012**, *380*, 1606.
- [6] C. N. Bernstein, *Am. J. Gastroenterol.* **2015**, *110*, 114.
- [7] B. R. R. De Mattos, M. P. G. Garcia, *Mediat. Inflamm.* **2015**, *2015*, 493012.
- [8] A. B. Pithadia, S. Jain, *Pharmacol. Rep.* **2011**, *63*, 629.
- [9] G. Bouguen, B. G. Levesque, *Clin. Gastroenterol. Hepatol.* **2015**, *13*, 1042.

- [10] R. J. Xavier, D. K. Podolsky, *Nature* **2007**, *448*, 427.
- [11] A. Sabbah, T. H. Chang, R. Harnack, V. Frohlich, K. Tominaga, P. H. Dube, Y. Xiang, S. Bose, *Nat. Immunol.* **2009**, *10*, 1073.
- [12] C. Wang, Y. Xiang, W. Ma, C. Guo, X. Wu, *Macromol. Biosci.* **2023**, 2300277.
- [13] L. L. Du, C. Ha, *Gastroenterol. Clin. N* **2020**, *49*, 643.
- [14] S. E. Berends, A. S. Strik, M. Lowenberg, G. R. D'Haens, R. A. A. Mathot, *Clin. Pharmacokinet.* **2019**, *58*, 15.
- [15] J. D. Feuerstein, K. L. Isaacs, Y. Schneider, S. M. Siddique, Y. Falck-Ytter, S. Singh, A. G. A. I. C. G. Comm, *Gastroenterology* **2020**, *158*, 1450.
- [16] X. Wang, J.-J. Yan, L. Wang, D. Pan, R. Yang, Y. Xu, J. Sheng, Q. Huang, H. Zhao, M. Yang, *Chem. Mater.* **2018**, *30*, 4073.
- [17] M. Gupta, V. Mishra, M. Gulati, B. Kapoor, A. Kaur, R. Gupta, M. M. Tambuwala, *Inflammopharmacology* **2022**, *30*, 397.
- [18] C. L. Xu, S. T. Chen, C. P. Chen, Y. C. Ming, J. H. Du, J. Y. Mu, F. Luo, D. Huang, N. Wang, Z. Y. Lin, Z. Q. Weng, *Int. J. Pharm.* **2022**, *623*, 121884.
- [19] M. A. Lebda, I. H. Elmassry, N. M. Taha, M. S. Elfeky, *Environ. Sci. Pollut. R* **2022**, *29*, 8294.
- [20] Y. Wang, Q. Tang, P. Duan, L. Yang, *Immunopharm. Immunot.* **2018**, *40*, 476.
- [21] T. Kusaba, *Clin. Med. Insights: Ther.* **2009**, *1*, CMT.S2096.
- [22] I. Khan, N. Ullah, L. J. Zha, Y. R. Bai, A. Khan, T. Zhao, T. J. Che, C. J. Zhang, *Pathogens* **2019**, *8*, 28.
- [23] M. Salice, F. Rizzello, C. Calabrese, L. Calandrini, P. Gionchetti, *Expert Rev. Gastroenterol. Hepatol.* **2019**, *13*, 557.
- [24] M. H. Zu, Y. Ma, *Adv. Drug Delivery Rev.* **2021**, *176*, 18.
- [25] D. Kalyane, N. Raval, R. Maheshwari, V. Tambe, K. Kalia, R. K. Tekade, *Mater. Sci. Eng., C* **2019**, *98*, 1252.
- [26] Y. Niu, Q. Xue, Y. Fu, *Macromol. Biosci.* **2021**, *21*, 2100162.
- [27] J. Yang, D. Li, M. Zhang, G. Lin, S. Hu, H. Xu, *J. Controlled Release* **2023**, *361*, 568.
- [28] J. R. Nakkala, Z. M. Li, *Acta Biomater.* **2021**, *123*, 1.

- [29] H. Q. Qiu, H. T. Gong, *Biomater. Sci.* **2022**, *10*, 457.
- [30] E. Gardey, F. H. Sobotta, S. Quickert, T. Bruns, J. C. Brendel, A. Stallmach, *Macromol. Biosci.* **2022**, *22*, 2100482.
- [31] G. Pasparakis, C. Tsitsilianis, *Polymer* **2020**, *211*, 16.
- [32] A. Sarode, A. Annapragada, *Biomaterials* **2020**, *242*, 15.
- [33] S. Hua, E. Marks, J. J. Schneider, S. Keely, *Nanomedicine* **2015**, *11*, 1117.
- [34] S. Y. Vafaei, M. Esmaeili, M. Amini, F. Atyabi, S. N. Ostad, R. Dinarvand, *Carbohydr. Polym.* **2016**, *144*, 371.
- [35] S. Chen, J. Wu, Q. Tang, C. Xu, Y. Huang, D. Huang, F. Luo, Y. Wu, F. Yan, Z. Weng, S. Wang, *Carbohydr. Polym.* **2020**, *228*, 115398.
- [36] J. Guo, H. Tao, Y. Dou, L. Li, X. Xu, Q. Zhang, J. Cheng, S. Han, J. Huang, X. Li, X. Li, J. Zhang, *Mater. Today* **2017**, *20*, 493.
- [37] N. G. Kotla, S. Rana, G. Sivaraman, O. Sunnapu, P. K. Vemula, A. Pandit, Y. Rochev, *Adv. Drug Delivery Rev.* **2019**, *146*, 248.
- [38] Å. Håkansson, N. Tormo-Badia, A. Baridi, J. Xu, G. Molin, M. L. Hagslätt, C. Karlsson, B. Jeppsson, C. M. Cilio, S. Ahrné, *Clin. Exp. Med.* **2015**, *15*, 107.
- [39] S.-B. Haange, N. Jehmlich, M. Hoffmann, K. Weber, J. Lehmann, M. von Bergen, U. Slanina, *J. Proteome Res.* **2019**, *18*, 1774.
- [40] D. Malhotra, A. L. Fletcher, S. J. Turley, *Immunol. Rev.* **2013**, *251*, 160.